

## Calculation of the localized and extended energy states density for $\text{Ge}_{60}\text{Se}_{40-x}\text{Te}_x$ alloy prepared by melting point method

J. H. Azzawi<sup>a</sup>, B. A. Ahmed<sup>b</sup>, K. A. Jasim<sup>b</sup>, E. M. T. Salman<sup>b,\*</sup>

<sup>a</sup>Directorate of Education, Diyala, Iraq

<sup>b</sup>Department of physics, College of Education for pure sciences Ibn Al-Haitham, University of Baghdad, Iraq

The DC electrical conductivity properties of  $\text{Ge}_{60}\text{Se}_{40-x}\text{Te}_x$  alloy with  $x = 0, 5, 10, 15$  and  $20$ ). The samples were formed in the form of discs with the thickness of  $0.25\text{--}0.30$  cm and the diameter of  $1.5$  cm. Samples were pressed under a pressure of  $6$  tons per  $\text{cm}^2$ , using a ton hydraulic press. They were prepared after being pressed using a ton hydraulic press using a hydraulic press. Melting point technology use to preper the samples. Continuous electrical conductivity properties were recorded from room temperature to  $475$  K. Experimental data indicates that glass containing  $15\%$  Te has the highest electrical conductivity allowing maximum current through the sample compared to Lu with other samples. Therefore, it is found that the DC conductivity increases with increasing Te concentration. The electrical conductivity properties show non-ohmic behavior due to the effects of temperature on the crystal structure of the samples, which indicates that the samples remain semi-conductive after partial replacement. Three conduction mechanisms are also observed for each sample at high, medium, and low temperatures. The Fermi level local and extended state densities and conductance parameters were calculated, and all were found to change with the change of Te concentration.

(Received May 8, 2023; Accepted September 4, 2023)

Keywords: Electrical conductivity, Alloy, Melting point technology, Partial replacement, Fermi level, Local and extended state densities

### 1. Introduction

The science of electronics entered into practice in all fields of science decades ago and began to develop very quickly [1]. Many electronic devices have been manufactured that depend in their work on materials with distinctive characteristics, which are semi-conductors that possess the properties of insulating materials at low temperatures, and the electrical conductivity increases when the temperatures rise to a certain extent. [2] Recently, research has expanded to identify the optical and electrical properties of semiconductors for the possibility of benefiting from them. This research has resulted in the manufacture of resistors, radar, transistors, solar cells, integrated electronic circuits, and electronic devices that are used in the fields of medicine, engineering, space exploration, chemistry, and the life sciences. [3] Semiconductor materials are characterized by the fact that electric charges in them move freely less than they are in conductive materials and that the specific electrical resistance of the semiconductor material lies between the specific resistance of the conductive and their ability to conduct electrically, i.e., within  $10^{-5}\text{--}10^{-8}$ . [4].

Semiconductors, by their nature, are either free from impurities such as germanium and silicon or doped with some materials to control their electrical conductivity. [5] The valence band for semiconductors in the degree of absolute zero is completely filled with electrons, and the conduction band is completely free of electrons. [6] When the temperature of the semiconductor was raised, some electrons moved from the valence band to the conduction band, which is ready for electrical conduction when an electric field is applied to it [7].

In pure semiconductors, fermi level is situated in center of limited energy gap. In amorphous semiconductors, there are edges that extend between the valence band and the

---

\* Corresponding author: [ibtisam.m.t@ihcoedu.uobaghdad.edu.iq](mailto:ibtisam.m.t@ihcoedu.uobaghdad.edu.iq)  
<https://doi.org/10.15251/CL.2023.209.649>

conduction band within the restricted energy gap; this in turn creates local states that overlap with each other within the energy gap; these states depend on the type of material. [8] To explain these confined states, scientists developed a number of models; Most famous of these models is Davis and Mote model, which adopted three processes to measure at high, medium, and low temperatures inside the energy gap, the electrical conductivity of amorphous semiconductors is a function of temperature.; these states are extended localized and fermi level. [9,10] Calculating the width of each band state from these equations:

$$\sigma = \sigma_{01}e^{(-\frac{\Delta E_1}{KT})} + \sigma_{02}e^{(-\frac{\Delta E_2}{KT})} + \sigma_{03}e^{(-\frac{\Delta E_3}{KT})} \quad (1)$$

where  $\sigma_{01}$ ,  $\sigma_{02}$  and  $\sigma_{03}$  are the conductivity of extended, localized, and Fermi level pre-exponential factor parameters, respectively; (T) is the absolute temperature; (KB) is Boltzmann's constant; and  $\Delta E_1$ ,  $\Delta E_2$  and  $\Delta E_3$  are the DC activation energies calculated from Slope  $\ln dc$  for the  $1000/T$  plot for each part[11,12].

The density of extended, localized, and Fermi levels has been studied by the researchers Aqeel N. Abdulateef et al.[13] studied how partial substitution of tin by indium at various concentrations affected variations in continuous electrical conductivity. The results showed that the density of located, extended fermi level states, activation energy, a change in tail width, and the distance of between the states decrease with increasing the addition of indium to  $Se_{85}Te_{10}Sn_{5-x}In_x$  alloy, and the distance of movement between states. Efforts of the researchers focused on studying the electrical properties of the alloy  $Se_{90-x}Te_5Sn_5In_x$  where the element Indium was added and the partial substitution of the element Selenium[14], they found that the activation energy increased in the glassy region and decreased in value in the crystalline region in the amorphous. The density of local and extended states as well as the Fermi level were analyzed as a result of the partial exchange of the trillium element in the alloy  $Ge_{30}Te_{70-x}Sb_x$  by the researchers [16]. It was concluded that a change occurred in all energy states, activation energy, tail width, interatomic distances, and the hoping transition distance[15]. The researchers focused on examining the electrical properties of the alloy  $Se_6Te_{4-x}Sb_x$  by partial substitution of selenium with antimony, where the shot density was calculated for different energy states (localize, extended, and Fermi level), the hopping distance between the electron, and the width of the tail. It was concluded that the energy densities changed with the increase in antimony concentration [12,16].

In this research, the partial substitution effect of selenium with trillium for the  $Ge_{60}Se_{40-x}Te_x$  alloy in different proportions (0, 5, 10, 15, and 20) will be studied on the density of states (localized, extended, and Fermi level) and its effect on the random energy level and the regularity of the crystal structure.

## 2. Experimental

The glassy alloys of  $Ge_{60}Se_{40-x}Te_x$  were prepared from germanium (Ge), selenium (Se), and tellurium (Te) prepared by quenching technology with high purity (99.999%), and weighed according to their atomic ratios. The addition of the element Te, which represents the variable concentration x, was prepared as follows: 0, 5, 10, 15, and 20 according to the chemical formula



All samples were weighed with a sensitive digital electrobalance. The proportions were mixed with each other and ground by hand for half an hour using an agate mortar after adding the alcohol solution. After that, they were ground with an electric mixer for an hour in order to homogenize them. Then, the samples were placed in an electric oven at 150 °C to get rid of moisture. The sample was formed into discs with a thickness of 0.25–0.30 cm and a diameter of 1.5 cm inside a hydraulic press under a pressure of 6 tons per square cm. The tablets were placed in a quartz glass tube, and the air was vacuumed and closed under a vacuum of  $10^{-4}$  degrees for hours at this temperature. After that, the ampoule is cooled to room temperature at the same rate at

which it was heated. It is crushed and samples are extracted after cooling. Then, using the same steps, it is re-ground and pressed into tablets that are kept in boxes and sent to the lab for the purpose of measuring the electrical resistance. After that, the electrical conductivity is measured as an indication of temperature.. Each sample was connected to a wire without resistance, and each sample was connected to electrodes using an ammeter and a voltmeter. The samples were placed in an electric oven by changing the temperature from room temperature to 180 °C. Current and voltage readings were taken at an average rate of every 10°C. The readings of the photometer V, ammeter I, and thermocouple T were recorded, and the resistance R, resistivity  $\rho$ , the thickness t and the conductivity  $\sigma$  were calculated as a function of temperature from the relationships:

$$R = \frac{V}{I} \quad (3)$$

$$\rho = \frac{RA}{t} \quad (4)$$

$$\sigma = \frac{1}{\rho} = \frac{t}{RA} \quad (5)$$

### 3. Result and discussion

After the  $\text{Ge}_{60}\text{Se}_{40-x}\text{Te}_x$  samples were placed in the electrical circuit, the voltage V and current I were calculated as a function of temperature. Equation 2 was used to compute the electrical resistivity R as a function of temperature. after the surface area and thickness of the samples have been substituted. the electrical resistivity  $\rho$  was calculated from Equation 3, and through the electrical resistance, Equation 4 was used to get the electrical conductivity D.C as an indicator of temperature. The relationship of  $\ln \sigma$  as a function of temperature is plotted for all  $\text{Ge}_{60}\text{Se}_{40-x}\text{Te}_x$  alloy samples, and x = 0, 5, 10, 15, and 20 values are shown in Fig. 1. For  $\text{Ge}_{60}\text{Se}_{40-x}\text{Te}_x$  alloy, a monotonous increase in continuous electrical conductivity was observed when the molar content of Te was increased from 0% up to 20% with an obvious increase at 15%.

The nonlinear current growth behavior of the current glasses indicates that the electrical properties tend towards non-ohmic behavior at the temperature applied across the sample [11-14]. The deviation of the ohmic behavior in the conductivity range is due to the effects of temperature in the sample. It is also evident from Fig. 1 that the electrical conductivity is higher for the  $\text{Ge}_{60}\text{Se}_{25}\text{Te}_{15}$  glass than for the other glasses in the  $\text{Ge}_{60}\text{Se}_{40-x}\text{Te}_x$  system (x = x = 0, 5, 10 and 20).

The electrical conductivity variation of  $\text{Ge}_{60}\text{Se}_{40-x}\text{Te}_x$  (x = x = 0, 5, 10, 15 and 20).chalcogenide glasses can be explained on the basis of changing the structure of these glasses with the addition of Te [11,12].

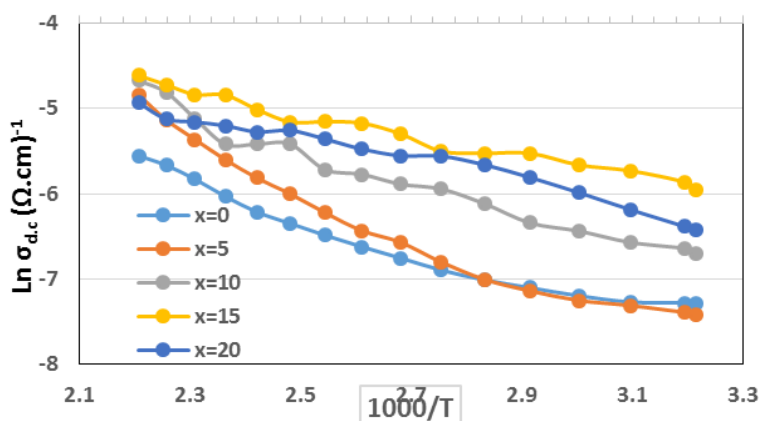


Fig. 1.  $\ln$  the electrical conductivity as an indicator of the temperature of glasses  $\text{Ge}_{60}\text{Se}_{40-x}\text{Te}_x$  with x = 0, 5, 10, 15 and 20.

From this figure, it is observed that changing the concentration of tellurium in the alloy results in a change in electrical conductivity. Curves were observed for each sample; these curves all contain three regions representing low, medium, and high temperatures, respectively. From these regions, the equation of each part of the curves has been derived, where the slope of the equation is  $\Delta E/k$  and the constant term is the point of intersection of the curve with the Y axis, which is represented in Figure. 1. From this values,  $\sigma_{01}$ ,  $\sigma_{02}$ ,  $\sigma_{03}$ ,  $\Delta E_1$ ,  $\Delta E_2$  and  $\Delta E_3$  were calculated as shown in Table 1.

*Table 1. The value of activation energies  $\Delta E_1$ ,  $\Delta E_2$  and  $\Delta E_3$  and the pre-exponential factors  $\sigma_{01}$ ,  $\sigma_{02}$ ,  $\sigma_{03}$  on the Te content of  $Ge_{60}Se_{40-x}Te_x$  alloy.*

Te	$\Delta E_1$ (ev)	$\sigma_{01}$	$\Delta E_2$ (ev)	$\sigma_{02}$	$\Delta E_3$ (ev)	$\sigma_{03}$
0	0.607	0.071	0.1672	0.021	0.0262	0.0065
5	0.869	0.0153	0.233	0.0162	0.0363	0.0078
10	0.479	0.0414	0.228	0.0044	0.0182	0.0055
15	0.499	0.0108	0.168	0.008	0.0243	0.0076
20	0.937	0.064	0.165	0.0417	0.0389	0.0053

Lone pair electrons, or unshared electron states, make up the valence band of the chalcogenide glass, which is abundant in group VI elements. Kastner first talked about the effects of adding elements to V-VI alloys. Because valence electrons close to electrically positive atoms would have higher energies than those adjacent to electrically neutral atoms, Kastne demonstrated that the presence of additives has an effect on the tails width  $\Delta E$  calculated through the difference between  $\Delta E_1$  and  $\Delta E_2$ , as shown in Figure (2). It was noted that the higher percentage of Te led to a change in the values of the tail width, as the increase in the width of the tail means an increase in randomness, while its decrease represents the change towards crystalline properties, and its results agree with the researchers in the source [15, 16].

The broadening of the valence band tail  $\Delta E$  [17]. Increasing the concentration of tellurium materials in the samples caused a change in the width of the tail of the valence band and conductivity, which caused a decrease in the energies of the electrically positive atoms at concentrations 10 and 20, This indicates that the concentration of tellurium 10 and 20 in the alloy [12]. while the concentration of tellurium 5 and 15 increased the valence electrons near the electrically positive atoms, which made the tail of the valence band widen. This indicates that the concentration of tellurium 5 and 20 in the alloy [15, 13].

The tail of the conduction band changes due to the increase or decrease of the types of bonds present in the alloy [9, 16]. Our findings, which are presented in Table 2, demonstrate how the broadening may not be symmetrical with the valence band and may result in an increase or decrease in the conduction band edge, which affects both the local state density  $N(E_{loc})$  and extended states  $N(E_{ext})$  at the Fermi level ( $E_F$ ).

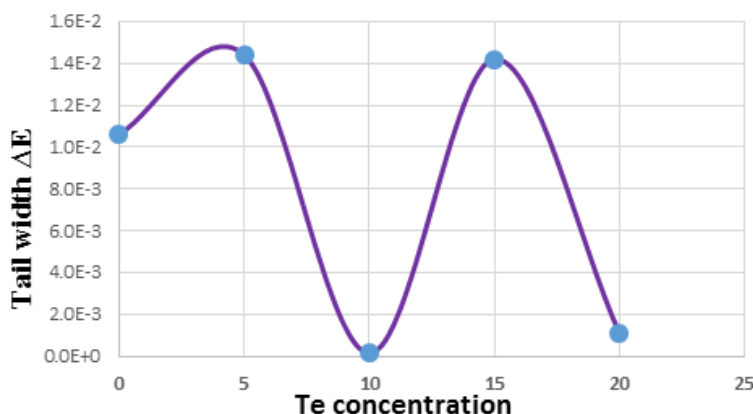


Fig. 2. Tail width of energy  $\Delta E$  as an indicator Te-concentration of  $Ge_{60}Se_{40-x}Te_x$  glasses.

Applying equation 5 below [11-13], the density of the extended state  $N(E_{ext})$  was computed for all samples after substituting the values of the constants ( $e$  is the electron charge,  $m$  is the electron mass, and  $h$  is the Planck's constant) and  $\sigma_{o1}$  parameters given from Table 1. It was discovered that changing the Te concentration causes the density of the extended states changing as well, and this is consistent with the results obtained by the researchers in reference [17]. The results are listed in Table 2.

$$N(E_{ext}) = \left[ \frac{6m}{e^2 h} \right] \sigma_{oext} \quad (5)$$

Using Equations 6 and 7 and the values of the constants (electron charge,  $V_{ph}$  phonon frequency =  $10^{13} \text{ s}^{-1}$ ,  $\sigma_{o2}$ ,  $\sigma_{o3}$ , and hopping distance between localization states  $R$ ), the local state densities at band tails and near to the Fermi level  $N(E_F)$  for all samples under experiment were calculated [18,19]. Table 2 summarizes the results.

$$N(E_{loc}) = \left[ \frac{6}{e^2 V_{ph} R^2} \right] \sigma_{oloc} \quad (6)$$

$$N(E_F) = \left[ \frac{6}{e^2 V_{ph} R^2} \right] \sigma_{o3} \quad (7)$$

$$R = 0.7736 \left\{ \frac{\Delta E a^{-1}}{N(E_{ext})(KT)^2} \right\}^{0.25} \quad (8)$$

where the width of energy is  $\Delta E = E_1 - E_2$ .

The hopping distance  $R$  was calculated from the equation 8 and values included in Table (2). The distance between atoms ( $a$ ) was calculated from the equation  $a = 0.025 / \sigma_o$ . All results are listed in Table 2.

Table 2. Represents Width fo tail  $\Delta E$ ,  $a$ ,  $R$ ,  $N(E_{loc})$ ,  $N(E_{ext})$ , and  $N(E_F)$  creation dependency as an indicator of Te content of  $Ge_{60}Se_{40-x}Te_x$  glasses with  $x = 0, 5, 10, 15$  and  $20$ .

x	Tail width $\Delta E$ (ev)	R( $\mu$ )	a ( $\mu$ )	$N(E_{ext.}) \times 10^{20}$ ( $ev^{-1}.cm^{-3}$ )	$N(E_{ext}) \times 10^{17}$ ( $ev^{-1}.cm^{-3}$ )	$N(E_{loc})$ ( $ev^{-1}.cm^{-3}$ ) $\times 10^8$
0	0.0106	0.0063	0.001084	20	32	11.7
5	0.0144	0.0194	0.071571	2.74	4.9	10.777
10	0.00018	0.0091	0.263245	5.71	1.3	1.2
15	0.0142	0.0212	0.101462	1.93	3.4	4.04
20	0.00111	0.0127	0.171261	1.49	2.2	1.16

Figure 3 represents the relationship between Tail Width  $\Delta E$ , the distance between atoms and the hopping distance  $R$  as a function of Te concentration. Table 2 shows the change in each of the values of  $\Delta E$ ,  $a$  and  $R$  as a function of Te concentration as they change due to a change in the size of the original and substituted atoms and the length of the bonds. Which is reflected in the purity of the alloy and the electrical properties [18].

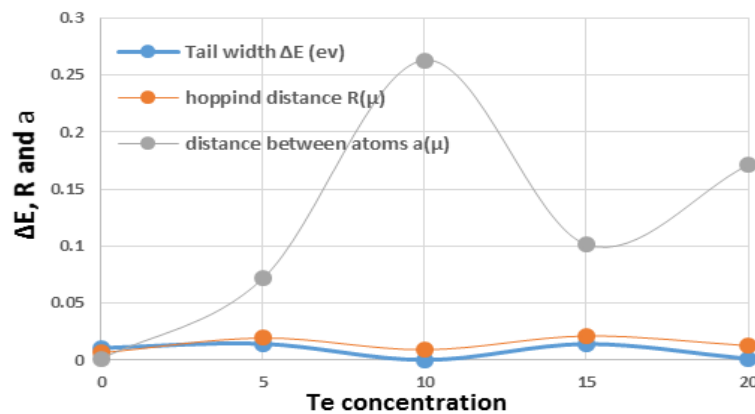


Fig. 3. Hopping transition distance  $R$ , Tail Width  $\Delta E$  and the spacing between atoms ( $a$ ) as a function of Te concentration for  $Ge_{60}Se_{40-x}Te_x$

After adjusting for the values of the constants in Table 1, the results in Table 2 were obtained for the densities of extended and localized states and Fermi level states, which were estimated for high, medium, and low temperatures using Equations 5, 6, and 7, respectively. reduction in states as shown in the figure 4, the expansion, localization, and Fermi level with increasing T concentration, as well as the decrease in energy levels, are caused by the rearrangement of atom bonding [19], the difference in atom sizes and valences between the original and substituted selves [20], and a reduce in the randomness of atoms' or molecules' structure of crystal in the  $Ge_{60}Se_{40-x}Te_x$  alloy.

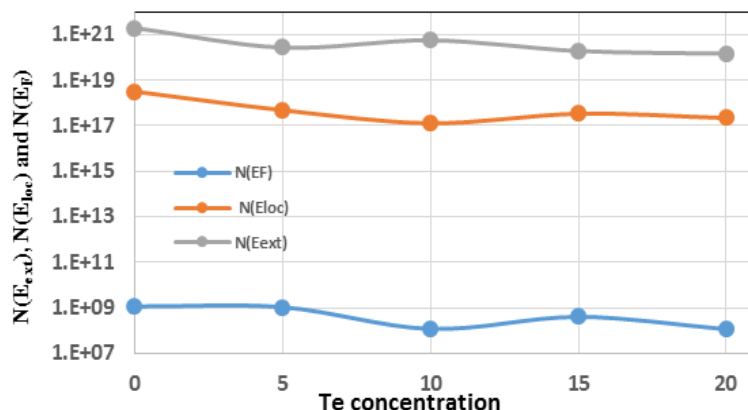


Fig. 4. Density of extended  $N(E_{ext})$ , localized  $N(E_{loc})$  and fermi  $N(E_F)$  states as function of Te content of  $Ge_{60}Se_{40-x}Te_x$  glasses with  $x = 0, 5, 10, 15$ .

#### 4. Conclusions

The melt point method was used for manufacturing five samples of the alloy  $Ge_{60}Se_{40-x}Te_x$  with  $x = 0, 5, 10, 15$  and 20. Electrical Conductivity was measured as an indicator of temperature, and it was found that there are three extended conduction regions, local levels, and Fermi levels at medium, low and high temperatures, respectively. Values of the extended, local and Fermi levels. It was also observed that the increase in the concentration of the tellurium element from  $x = 0$  to 15 decreased in this region and increased in  $x = 10$  and then decreased in  $x = 20$ .

#### References

- [1] Rajesh, R., Philip, J. (2003), Semiconductor Science and Technology, 18(2), 133-138; <https://doi.org/10.1088/0268-1242/18/2/312>
- [2] Tanaka, K. (1989), Physical Review B, 39(2), 1270-1279; <https://doi.org/10.1103/physrevb.39.1270>
- [3] Mahdi, S. H., Jassim, W. H., Hamad, I. A., Jasim, K. A. (2017), Energy Procedia, 119, 501-506; <https://doi.org/10.1016/j.egypro.2017.07.059>
- [4] Kern, K., & Känel, H. V. (2004), Applied Physics Letters 85(23), 5673-5675; <https://doi.org/10.1063/1.1829164>
- [5] Mahdi, H. A., Jasim, K. A., & Shaban, A. H. (2019), Energy Procedia, 157, 158-163. <https://doi.org/10.1016/j.egypro.2018.11.176>
- [6] Márquez, J., Stange, H., Hages, C. J., Schaefer, N., Levchenko, S., Giraldo, S., Saucedo, E., Schwarzburg, K., Abou-Ras, D., Redinger, A., Klaus, M., Genzel, C., Unold, T., & Mainz, R. (2017), Chemistry of Materials 29(21), 9399-9406; <https://doi.org/10.1021/acs.chemmater.7b03416>
- [7] Jasim, K. A. (2013), Turkish Journal of Physics, <https://doi.org/10.3906/fiz-1203-16>
- [8] Radhi Jobayr, M., Mahdi, S. H., Salman, E. M., & Jasim, K. A. (2022), Journal of Ovonic Research, 18(3), 357-371. <https://doi.org/10.15251/jor.2022.183.357>
- [9] Khudhair, N. H., & Jasim, K. A. (2023), Ibn AL-Haitham Journal For Pure and Applied Sciences, 36(1), 149-157; <https://doi.org/10.30526/36.1.2892>
- [10] Sharma, N., Sharma, S., Sarin, A., Kumar, R. (2016), Optical Materials, 51, 56-61; <https://doi.org/10.1016/j.optmat.2015.11.021>
- [11] Majeed, Z. N., Dahaher, N. N., & Alwan, E. K. (2021), MINAR International Journal of Applied Sciences and Technology, 03(02), 100-108; <https://doi.org/10.47832/2717-8234.2-3.13>

- [12] Ahmed, B. A., Mohammed, J. S., Fadhil, R. N., Jasim, K. A., Shaban, A. H., Al Dulaimi, A. H. (2022), Chalcogenide Letters, 19(4), 301-308; <https://doi.org/10.15251/cl.2022.194.301>
- [13] Abdulateef, A. N., Alsudani, A., Chillab, R. K., Jasim, K. A., Shaban, A. H. (2020), Journal of Green Engineering (JGE), 10(9), 5487-5503.
- [14] Ram, I. S., Kumar, S., Singh, R. K., Singh, P., Singh, K. (2015), AIP Advances, 5(8), 087164; <https://doi.org/10.1063/1.4929577>
- [15] Chillab, R. K., Jahil, S. S., Wadi, K. M., Jasim, K. A., Shaban, A. H. (2021), Key Engineering Materials, 900, 163-171; <https://doi.org/10.4028/www.scientific.net/kem.900.163>
- [16] Baker, E. H., Webb, L. M. (1974), Journal of Materials Science, 9(7), 1128-1132; <https://doi.org/10.1007/bf00552828>
- [17] Kastner, M. (1972), Physical Review Letters, 28(6), 355-357; <https://doi.org/10.1103/physrevlett.28.355>
- [18] Aleabi, S. H., Watan, A. W., Salman, E. M., Jasim, K. A., Shaban, A. H., & AlSaadi, T. M. (2018), AIP Conference Proceedings. <https://doi.org/10.1063/1.5039178>
- [19] Khudhair, N. H., Jasim, K. A. (2023), Technologies and Materials for Renewable Energy, Environment and Sustainability; <https://doi.org/10.1063/5.0129373>
- [20] Khudhair, N. H., Jasim, K. A. (2023), Technologies and Materials for Renewable Energy, Environment and Sustainability; <https://doi.org/10.1063/5.0129550>